EAN 2024 62nd annual conference on experimental stress analysis

Experimental Study of Fundamental Mechanical Properties of Ultra-Thin 3D-Printed Titanium Alloy with Beta Structure

A. Jíra[1,*], Z. Tolde[2], J. Fojt[3]

[1] *Czech Technical University in Prague, Faculty of Civil Engineering, Department of Mechanics, Czech Republic*

[2] *Czech Technical University in Prague, Faculty of Mechanical Engineering, Department of Physics, Czech Republic*

[3] *University of Chemistry and Technology Prague, Faculty of Chemical Technology, Department of Metals and Corrosion Engineering, Czech Republic*

[*] *jira@fsv.cvut.cz*

Abstract: 3D printing of beta-titanium alloys for biomedical applications is currently in high demand, both for material reasons and for the ability to produce highly complex replacements, often directly tailored to the patient. These individual implants require a porous surface that is printed from thin parts at the limits of the 3D printer's capabilities. The thin structures are then very susceptible to changes in mechanical properties due to poor print quality, and building a corresponding numerical model is very complicated. The aim of this work is to experimentally describe the basic mechanical properties of thin 3D-printed titanium alloy samples with a beta structure. These values can then serve as input quantities for numerical modeling via particle models.

Keywords: 3D printing; surface etching; titanium alloy; porosity; mechanical testing.

1 Introduction

In the past decade, there has been a revolutionary transformation in manufacturing due to 3D printing, enabling the creation of intricate structures with high precision. In biomedicine, this technology has become pivotal for the development of implants and joint replacements that can better match individual anatomical characteristics of patients [1, 2]. The key advantage of using 3D printing with these materials lies in the utilization of complex porous structures, such as gyroid-based designs [3], which ensure optimal integration of the implant with surrounding bone tissue. However, these structures are often very thin (typically 150 – 600 μm), pushing the limits of current printers and the powders used.

A critical factor for a successful 3D-printed implant is the material used and its biomechanical reliability. Most current replacements are made from the titanium alloy Ti6Al4V, which is well-proven and has been used for a long time. However, it also has disadvantages, such as a high Young's modulus and potential toxicity, making it worth considering alternatives. Possible replacements include beta-structured titanium alloys, such as Ti25Nb4Ta8Sn [4, 5, 6]. The Ti25Nb4Ta8Sn alloy is bioactive, non-cytotoxic, and serves as a suitable alternative to the widely used Ti6Al4V alloy in terms of mechanical properties and corrosion resistance [7]

In real-world applications, experimental measurements often do not correspond with numerical models due to internal material porosity and incomplete fusion of powder particles at the structure's edges [8].

This work serves as a pilot study on the behavior of thin 3D printed samples, aiming to experimentally assess their mechanical properties. The values obtained will form the basis for creating a numerical model. Numerical modeling and simulations are crucial for precise design and optimization of these structures based on desired mechanical properties.

2 Methodology

Sample preparation was focused on 3D printing (type Dog bone) specimens for uniaxial tensile testing to obtain fundamental material characteristics for subsequent numerical modeling. For this purpose, both conventional titanium alloy Ti6Al4V and an experimental alloy Ti25Nb4Ta8Sn were utilized. The Ti6Al4V specimens underwent surface etching, while the Ti25Nb4Ta8Sn specimens were evaluated in different groups:

- Group I: Ti25Nb4Ta8Sn samples without supplementary post-processing treatments.
- Group II: Ti25Nb4Ta8Sn samples subjected to post-annealing to alleviate internal stresses.
- Group III: Ti6Al4V specimens without additional post-processing treatments.
- Group IV: Ti6Al4V samples subjected to surface etching and removal of imperfectly fused powder grains through washing.

These experimental groups were essential for evaluating and comparing the mechanical properties and structural integrity of the printed specimens under different conditions.

2.1 Preparation of samples

Groups III and IV samples were produced using the SLM technique from Ti6Al4V titanium alloy (Rematitan CL) with a maximum grain size of 63 μm. These samples were fabricated in collaboration with ProSpon, Ltd. (Kladno, Czech Republic) using an M2 Cusing machine. The 3D printing was conducted in an argon environment with 0.5% oxygen maintained within the welding chamber. After printing, the samples underwent thermal processing under vacuum to relieve internal stresses, involving gradual heating to 840 °C over 4 hours, holding at 840 °C for 2 hours, and then cooling to room temperature. Additionally, samples from group IV were subjected to chemical etching to remove imperfectly fused powder [9] particles.

For 3D printing samples from groups I and II, Ti25Nb4Ta8Sn alloy powder with a particle size range of 10-120 μm and an average particle size of 50 μm, supplied by Advanced Metal Powders s.r.o., was used. The selective laser melting (SLM) method was employed for 3D printing the beta-titanium alloy in collaboration with the Institute of Physics of the Czech Academy of Sciences, followed by thermal treatment in cooperation with UJP Prague. The samples were annealed at 1000 °C for 1 hour and then gradually cooled in the furnace.

2.2 Mechanical testing in uniaxial tension

Mechanical testing was conducted using a LiTeM machine (Italy). Dog bone-shaped specimens (Fig. 1) from groups I-IV were produced with thicknesses of 500, 750, and 1000 μm and subjected to uniaxial tensile testing. The test parameters were chosen according to EN 10993 standards, considering the potential future use for implants. The test was performed in controlled displacement mode at a rate of 0.04 mm/min.

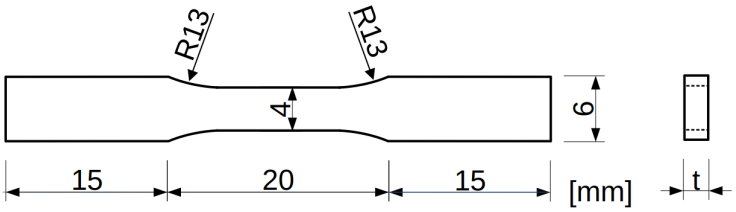

Fig. 1: The geometry of dog bone-shaped test specimens for uniaxial tensile testing features a thickness (t) determined by the printing capabilities, set in increments of 250 μm.

Results

As a basic comparison to illustrate the development of mechanical properties of thin samples, uniaxial tensile testing was performed. The graphs in Fig. 2 show representative force-displacement curves for different sample thicknesses (t). The Ti25Nb4Ta8Sn alloy samples were tested on five specimens without subsequent processing (blue line) and on five specimens that underwent annealing to remove internal stresses (red line). The Ti6Al4V alloy samples were tested on five specimens without additional treatment (blue line) and on five specimens after etching to remove imperfectly welded powder particles (green line).

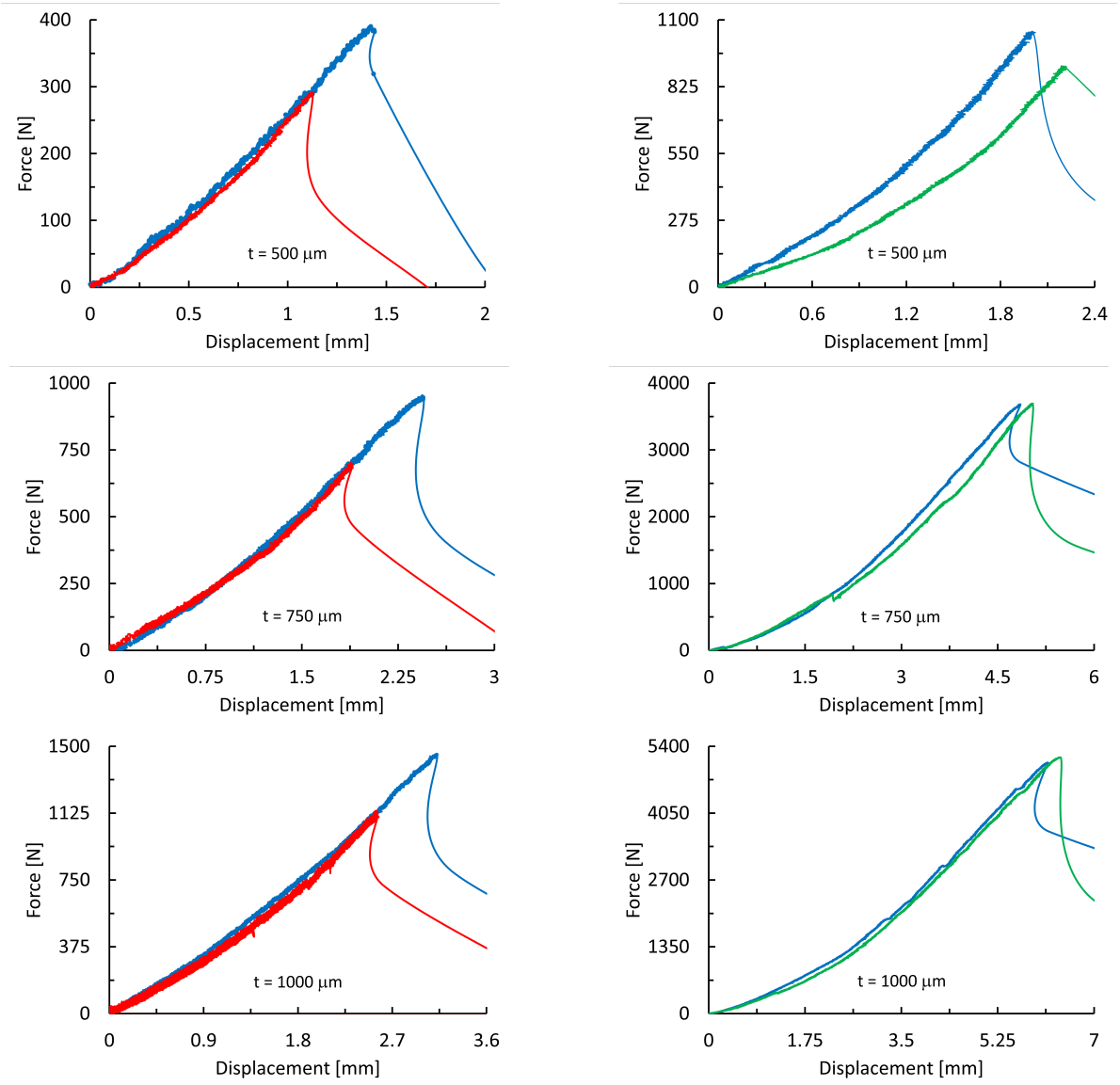

Fig. 2: Graphs depicting the force-displacement relationship from uniaxial tensile testing for materials Ti25Nb4Ta8Sn (left column) and Ti6Al4V (right column). Ti25Nb4Ta8Sn without subsequent processing – blue line, Ti25Nb4Ta8Sn with annealing – red line. Ti6Al4V without additional treatment – blue line, Ti6Al4V after etching – green line.

The standard Ti6Al4V alloy exhibits significantly higher tensile strength compared to the Ti25Nb4Ta8Sn alloy (Tab. 1). This difference can be attributed to the significantly higher porosity in the beta-structured alloy. This high porosity also leads to a substantial reduction in strength after annealing, although there is no significant change in Young's modulus. In contrast, the conventional alpha-beta alloy did not show a decrease in tensile strength in the etched samples, but a significant decrease in Young's modulus was observed in the thinnest samples based on the graphs. As thickness increases, the differences in the force-displacement curves diminish, indicating that the quality of 3D printing plays a less decisive role.

The failure of the samples during uniaxial tensile testing mainly occurred along the grain boundaries. Additionally, a significant number of imperfectly melted powder particles were observed, resulting in very low tensile strength and fracture forces (Fig. 3). This phenomenon was only observed in the Ti25Nb4Ta8Sn alloy, which the authors attribute to incorrect printing settings. Optimization of printing parameters will be the subject of further investigation and is not part of this study. However, for the purposes of numerical modeling and particle model development, this high porosity is advantageous as it allows for more detailed particle modeling.

The values of the Young's modulus can be determined from the graphs in Fig. 2. The average values range from 3600 to 3900 MPa for the Ti25Nb4Ta8Sn alloy (for thicknesses of 500 to 1000 μm). In comparison, the modulus of elasticity for the Ti6Al4V alloy is in the range of 7000 to 8000 MPa. Post-processing modifications

t [μm]		Ti25Nb4Ta8Sn with annealing	Ti25Nb4Ta8Sn without annealing	Ti6Al4V with etching	Ti6Al4V without etching
500	F_{max} [N]	407.5 $\pm$ 11.8	207.7 $\pm$ 29.6	1009.4 $\pm$ 43.5	760.0 $\pm$ 85.4
	σ_{max} [MPa]	203.8 $\pm$ 5.9	135.3 $\pm$ 14.8	504.7 $\pm$ 21.8	380.3 $\pm$ 75.0
750	F_{max} [N]	889.6 $\pm$ 38.6	674.0 $\pm$ 86.1	3570.4 $\pm$ 129.5	3571.1 $\pm$ 105.8
	σ_{max} [MPa]	296.5 $\pm$ 12.9	224.7 $\pm$ 28.7	1190.1 $\pm$ 83.2	1190.4 $\pm$ 61.9
1000	F_{max} [N]	1442.6 $\pm$ 69.9	1010.9 $\pm$ 101.0	4579.4 $\pm$ 177.1	4958.9 $\pm$ 133.0
	σ_{max} [MPa]	360.6 $\pm$ 16.7	252.7 $\pm$ 25.3	1144.9.7 $\pm$ 144.9	1246.5 $\pm$ 45.7
		Group I	Group II	Group III	Group IV

Tab. 1: Average values of yield strength and ultimate tensile strength for different types of samples.

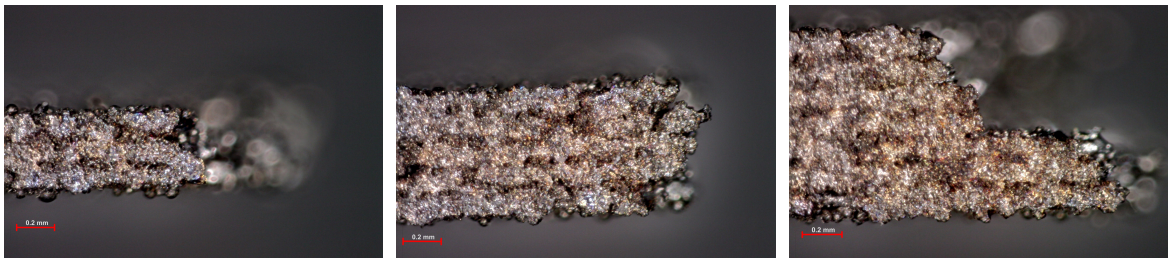

Fig. 3: Samples from group I with thicknesses of 500, 750, and 1000 μm showed visible internal structures due to imperfect 3D printing.

have a negligible effect on the resulting modulus of elasticity.

3 Conclusions

Uniaxial tensile testing was conducted as a fundamental comparison to illustrate the development of mechanical properties in thin samples. The standard Ti6Al4V alloy exhibits significantly higher ultimate tensile strength values compared to the Ti25Nb4Ta8Sn alloy. This difference can be attributed to the significantly higher porosity in the beta-structured alloy. This high porosity ($\sim$16–19 %) also leads to a substantial reduction in strength after annealing, although there is not a notable change in the Young's modulus. Conversely, for the conventional alpha-beta alloy, there was no decrease in ultimate tensile strength for etched samples, but significant decreases in Young's modulus were observed for the thinnest samples. As the thickness increases, the differences in the force-displacement curves diminish, suggesting that the quality of 3D printing plays a less critical role.

Acknowledgement

We are thankful for financial support provided by The Czech Science Foundation (GACR) grant No. 23-04971S and Czech Technical University in Prague grant SGS No. SGS23/152/OHK1/3T/11.

References

[1] D. Serrano, et al., 3D Printing Technologies in Personalized Medicine, Nanomedicines, and Biopharmaceuticals, Pharmaceutics. vol. 15 (2023).

[2] B. Li, et al. Application and Development of Modern 3D Printing Technology in the Field of Orthopedics, BioMed Research International. vol. 2022 (2022) 1-15.

[3] A. Jíra, et al., Variability of the Gyroid Structure for Biomedical Applications, 59th International Scientific Conference on Experimental Stress Analysis, Litomyšl, Czech Republic, 2021.

[4] Z. Tolde, V. Starý, L. Cvrček, M. Vandrovcová, J. Remsa, S. Daniš, Growth of a TiNb adhesion interlayer for bioactive coatings, Materials Science and Engineering: C. vol. 80 (2017). https://doi.org/10.1016/j.msec.2017.07.013.

[5] M. Vandrovcova, Z. Tolde, P. Vanek, V. Nehasil, M. Doubková, M. Trávníčková, J. Drahokoupil, E. Buixaderas, F. Borodavka, J. Novakova, L. Bacakova, Beta-Titanium Alloy Covered by Ferroelectric Coating–Physicochemical Properties and Human Osteoblast-Like Cell Response, Coatings. vol. 11 (2021). https://doi.org/10.3390/coatings11020210.

[6] I. Jirka, M. Vandrovcová, O. Frank, Z. Tolde, J. Plšek, T. Luxbacher, L. Bačáková, V Starý, On the role of Nb-related sites of an oxidized β-TiNb alloy surface in its interaction with osteoblast-like MG-63 cells, Materials Science and Engineering: C. vol. 33 (2013) 1636-1645. https://doi.org/10.1016/j.msec.2012.12.073.

[7] V. Hybasek, J. Fojt, J. Malek, E. Jablonska, E. Pruchova, L. Joska, T. Ruml, Mechanical properties, corrosion behaviour and biocompatibility of TiNbTaSn for dentistry, Materials Research Express. vol. 7 (2020) 13. https://doi.org/10.1088/2053-1591/ab62f7.

[8] A. Jíra, et al., Mechanical Properties of Porous Structures for Dental Implants: Experimental Study and Computational Homogenization, Materials. vol. 14 (2021).

[9] J. Fojt, Z. Kacenka, E. Jablonska, V. Hybasek, E. Pruchova, Influence of the surface etching on the corrosion behaviour of a three-dimensional printed Ti–6Al–4V alloy, Materials And Corrosion. 71 (2020) 1691-1696. https://doi.org/10.1002/maco.202011658

[10] EN ISO 10993 standards – Testing of Medical Devices.